Effect of length scales in directing step bunch self-organization during annealing of patterned vicinal Si(111) surfaces: Comparison with a simple near-equilibrium model

Hung-Chih Kan,[1,3,*] Taesoon Kwon,[2,3] and R. J. Phaneuf[1,2,3]
[1]*Department of Physics, University of Maryland, College Park, Maryland 20742, USA*
[2]*Department of Materials Science and Engineering, University of Maryland, College Park, Maryland 20742, USA*
[3]*Laboratory for Physical Sciences, University of Maryland, College Park, Maryland 20740, USA*
(Received 16 January 2008; published 1 May 2008)

We compare the experimental observations of the effect of changing the length scale of an artificially imposed pattern on self-organization during annealing of stepped Si(111) surfaces with the predictions of the simple quasi-one-dimensional near-equilibrium model proposed by Weeks *et al.* [*Dynamics of Crystal Surfaces and Interfaces*, edited by P. Duxbury and T. Spence (Plenum, New York, 1997), pp. 199–216] in which step stiffness competes with the effect of repulsive step-step interactions. We find that this model reproduces the observed convergence of in-plane and out-of-plane relaxation at large length scales, but faster relaxation in plane at small periods. Simulations based on this model require step energetic parameters which dramatically depart from their equilibrium values to obtain agreement with the observed pattern period at which relaxation becomes isotropic. We find that this model does not reproduce the observed asymptotic quartic dependence of the relation time on spatial period.

DOI: 10.1103/PhysRevB.77.205401 PACS number(s): 81.16.Dn, 68.35.Md

Self-organization in nature often leads to pattern formation at characteristic length scales, a phenomenon which has long fascinated scientists. It also presents a clue as to how bottom-up fabrication of densely packed arrays of nanometer scale structures might be practically achieved. A potential approach would use an initial artificially defined pattern to set conditions for the physical driving forces which control evolution during a subsequent sample processing step. A first step toward directing self-organization would be a quantitative understanding of the competing physical mechanisms involved, and, in particular, how these interactions vary with lateral length scale. Systems for which such a quantitative understanding exists, however, are rare.

In this report, we examine a system in which self-organization shows an intriguing dependence on length scale which can be explored through the introduction of an artificially imposed pattern: stepped Si(111) surfaces.[1–4] While there have been a number of reports of how lithographically patterned surfaces evolve during growth or annealing,[1–3] only recently have there been systematic investigations of the effect of the characteristic pattern length scale in directed self-organization of semiconductor surfaces.[4–7] Elsewhere we reported experimental observations of the structures that result from patterning stepped Si(111) surfaces during annealing, in which we found that introducing topographical features at a chosen length scale can steer the interplay between these driving forces, leading to distinct paths of evolution with qualitatively different intermediate surface morphologies.[5] Here, we compare these observations with the predictions of a simple model[8] in which steps move across the surface under the influence of step stiffness, the interactions between steps, and sublimation; we find that agreement between this model and experiment requires the interaction parameters to dramatically depart from their equilibrium values.

We begin with a brief description of the experiments and experimental results, discussed in more detail elsewhere.[5] We patterned vicinal Si(111) wafers, oriented by $0.5 \pm 0.25°$, toward [$\bar{2}$11], using photolithography and reactive ion etching to create arrays of cylindrically shaped pits on the surface whose diameter we systematically varied from 0.7 to 8.0 μm, and whose center-to-center spacing was twice the pit diameter; the depth of the pits after etching was approximately 32 nm. The patterned samples were introduced into ultrahigh vacuum, and heated from behind using a combination of radiation and electron bombardment; this procedure eliminates the electromigration effects which result from resistive heating.[11–13,15] Following extensive outgassing at a temperature of $\sim$600 °C, the samples were heated to a temperature of 1273 ± 5 °C for varying periods of time, varying between 30 s and several minutes. We used a disappearing-filament pyrometer in measuring this temperature; this placed a lower limit of $\sim$30 s on reliably determined annealing times. We then quench cooled the samples, and transferred them through atmosphere into a commercial atomic force microscope for imaging.

Our atomic force microscopy (AFM) images showed that the shortest annealing studied produce a disappearance of the pits on the smaller period structures; in agreement with reports by Ogino,[1] they are replaced by arrays of nearly straight step bunches whose spatial period matches that of the initial pattern. Not surprisingly, the annealing time required for the disappearance of the pits monotonically increases with the initial pit diameter. More interesting is the behavior during continued annealing, subsequent to the disappearance of the pits which reveals a richness in the mode of self-organization of the step bunches as the spatial period is varied. While both the "waviness" of the step bunches (i.e., the amplitude of the topographical corrugation within the average surface plane) and their height exponentially decay with time subsequent to the disappearance of the last circular "loop" steps, there is a pronounced difference in the length-scale dependence of the two types of relaxation times. The in-plane relaxation time shows an approximate fourth-

order power law dependence on lateral period, in agreement with Mullins' famous prediction.[10] The dependence of the out-of-plane decay time on spatial period is more complicated: for short period structures, the relaxation time out of plane is considerably longer than in plane; however, with increasing spatial period, the out-of plane and in-plane decay times converge. In other words, the step bunch waviness and height anisotropically decay for small patterns, but isotropically in the large period limit.

In this report, we examine whether it is possible to understand this length scale dependence of the pattern evolution in terms of a simple model of step motion and interactions; we carry out numerical simulations based on the specific model proposed by Weeks *et al.*,[8] which we briefly review here. The model is based on the supposition that the step motion can be written in terms of the surface free energy. Following Gruber and Mullins,[9] in equilibrium the surface free energy per projected area for a vicinal surface can be written in terms of the slope s as

$$f(s) = f_0 + \frac{\beta}{h}s + gs^3, \tag{1}$$

where f_0 is the free energy per area for the flat surface, β is the step creation free energy per length, h is the step height, and g measures the strength of the step-step interactions, which include both entropic and elastic effects. For stepped Si(111) surfaces, the nature of these driving forces has been extensively studied over a range of temperature.[11–15] Near equilibrium, the step dynamics are expected to be controlled by variations in the effective two dimensional step Hamiltonian, which can be written as[8]

$$H(\{x_n\}) = \int dy \sum_n^{N_s} \left[\frac{\tilde{\beta}}{2}\left(\frac{\partial x_n(y)}{\partial y}\right)^2 + V[w_n(y)] \right], \tag{2}$$

where the summation is over all steps and the integration is along a given step. The first term corresponds to the free energy associated with distorting an individual step, and is proportional to the step stiffness $\tilde{\beta}$, while the second term takes into account the step-step interactions. In the model proposed by Weeks *et al.*, only the interactions between near-neighbor steps are considered, and the interaction is written in terms of the terrace width, $w_n \equiv x_{n+1}(y) - x_n(y)$. Both interactions with more distant steps and the interaction between segments of adjacent steps with different values of y are omitted in this simple model. For a small change in the lateral position of the nth step $\Delta x_n(y)$, the change in the Hamiltonian is approximately given by the integral over the length of the step of the product of this displacement and the functional derivative $\delta H / \delta x_n(y)$. Using this, the step chemical potential is written as

$$\mu_n(y) = \Omega \left[\frac{\partial V(w_n)}{\partial w_n} - \frac{\partial V(w_{n-1})}{\partial w_{n-1}} + \tilde{\beta}\frac{\partial^2 x_n}{\partial y^2} \right], \tag{3}$$

where Ω is the area occupied by an atom. The first two terms in brackets in this expression correspond to the pressure exerted by the step by the adjacent terraces, and the last term is proportional to the linearized curvature of the step. The velocity of the step can now be written using a linear kinetics approximation, taking the effective mass flow to be nonlocal, so that atoms are exchanged between the step edge and a reservoir, whose chemical potential is zero in the absence of step motion. Finally, an additional, driving term in the step velocity corresponds to sublimation, which is significant at the temperature at which we anneal the patterned surfaces. This should be proportional to the widths of the adjacent terraces, at least as long as the diffusion length exceeds these; allowing for a possible asymmetry in the probability of an atom moving from a step onto the terraces above and below gives the following expression for the velocity of a step in this model:

$$\frac{d\vec{S}}{dt} = \frac{\hat{n}\cdot\Gamma}{k_B T}\left(\frac{\tilde{\beta}}{R} + gh^3\left(\frac{1}{w_1^3} - \frac{1}{w_2^3}\right)\right) - \hat{n}\cdot(k^- \cdot w_1 + k^+ \cdot w_2), \tag{4}$$

where $\vec{S}$ is the trace of an individual step projected in the (111) plane, $\hat{n}$ is the local normal of the step edge within the (111) plane, Γ is the step mobility, k_B is Boltzmann's constant, T is the surface temperature, $\tilde{\beta}$ is the step stiffness, R is the local radius of curvature of the step edge, g is the step-step interaction coefficient, h is the step height, $w_1(w_2)$ is the distance to nearest neighboring uphill-(downhill)-side step, measured along $\hat{n}$, and $k^+(k^-)$ is the Si adatom attachment/detachment rate at the step edge from the step down (up) terrace.

An important question is whether a near-equilibrium model like that described above can be used in understanding step motion when sublimation is significant. To address this, in the results presented below, we integrate Eq. (4) using the finite difference method, with periodic boundary conditions, and compare its prediction with our experimental observations. At the downhill-side pit edge, the outermost loop step and the neighboring vicinal step have opposite signs. This results in the possibility of both a nonrepulsive step interaction and step annihilation when they touch. For simplicity, we flip the sign of g to calculate the step-step interaction for this case, and allow crossing and annihilation between these two steps; effectively, this "transfers" a neighboring vicinal step across the pit. We see no evidence for the Ehrlich-Schwoebel effect[16] in the experiment;[5] we thus set $k^+ = k^-$. We discuss the parameters used in the simulations below.

NUMERICAL RESULTS

Figures 1(a)–1(c) show the initial step configurations within the three unit cells, centered about circular pits of successively larger diameter. As in the experiment, we set the center-to-center spacing between the pits at twice the initial diameter, and the depth of the pits at ~35 nm, measured along the vicinal surface normal. The reactive ion etching process we experimentally use produces pits with nearly vertical sidewalls; however, for ease of simulation, we reduce the inclination angle of the sidewalls in the starting geometry to 15°. The vertical lines colored in red represent steps which result from the sample miscut, which we refer to as "vicinal

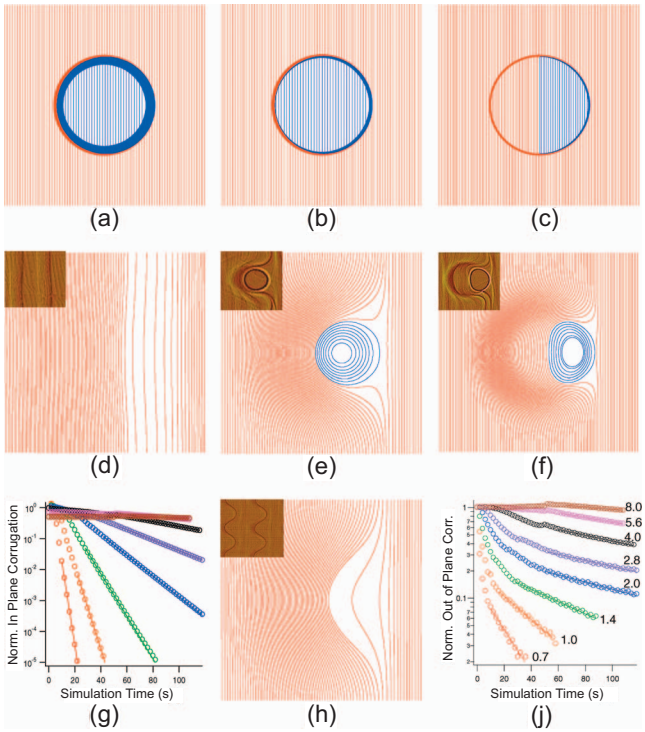

FIG. 1. (Color) Simulated evolution of step structure on vicinal Si(111) surfaces. [(a)–(c)] Initial step configurations for pit diameters equal to 1.4, 4, and 8 μm, respectively. [(d)–(f)] Step structure for panels (a)–(c), respectively, after 30 s simulation time. (h) Step structure for 4 μm initial pit diameter after 60 s simulation time. Field of view for panels (a) and (d) is 2.8 μm, 8 μm for panels (b), (e), and (h), and 16 μm for panels (f) and (j). For visibility, only a fraction of the steps are shown here. Step-up direction horizontally points to the left. Insets in panels (d)–(f) and (h) are high-pass filtered AFM images scanned from real sample after corresponding annealing time (Ref. 5). Panels (g) and (j) show the in-plane and out-of-plane corrugations, respectively, measured from the simulation as a function of simulation time for each pit size, with the color vs pit size indicated in (j).

steps"; based on a vicinal angle of 0.5° the average spacing of these is 36.5 nm. Vicinal steps interfering with the pit structure bend around the uphill edge of the pit and become part of the sidewall. The curves colored in blue represent steps created by the patterning, which we refer to as "loop steps." For the smaller patterns, the pit structure consists almost entirely of contiguous loop steps, with only a few vicinal steps within the uphill sidewall. For the largest initial diameter of 8 μm, because of the shallowness of the pit and the finite angle that the surface makes with respect to the (111) terraces, both vicinal steps and loop steps make a significant contribution to the starting pit structure.

Figures 1(d)–1(f) show the simulated step morphology after 30 s of simulated annealing, based on integration of Eq. (4) with a time step of 10 μs. For the smallest pattern shown here, the initial pit diameters are 1.4 μm; all loop steps have by this time disappeared, and a straight step bunch has formed at the uphill side of the original pit. During the first 10 s of evolution, almost all of the loop steps evolve into nearly circular, concentric rings, shrink inward, and self-annihilate one by one into the center. Only a few of the outer loop steps annihilate with approaching vicinal steps. Instead, for the smaller period structures, the effect of step stiffness dominates the evolution, driving the Si adatoms to fill in the circular "void islands" despite the competing influence of the sublimation of adatoms. After all loop steps disappear, the stiffness results in further relaxation, and a rapid formation of nearly straight step bunches. For the intermediate-size pattern shown in Fig. 1(b), with 4 μm initial pit diameters, the loop steps are by 30 s nearly circular and concentric. The innermost loop steps initially shrink and disappear here as well, but this ceases at the point at which the innermost surviving loop step is large enough that sublimation balances the effect of step stiffness. The outer loop steps in this case expand outward and locally annihilate with vicinal steps which approach from the downhill side. As shown in Fig. 1(e), a few circular loop steps remain after 30 s of annealing, with those vicinal steps which annihilated at the downhill edge bending around the uphill edge and adding to curved step bunches. For the largest pattern, 8 μm initial pit diameters, half of the initial sidewall consists of vicinal steps. Their presence causes the innermost loop steps to be nearly flat on the uphill side. In addition, relaxation of steps at the original uphill wall produces an extended curved bunch across the original wall position. For these largest pits, the simulation shows that an even larger portion of the loop steps annihilate with approaching vicinal steps, rather than shrinking and disappearing. Figure 1(h) shows that with further simulated annealing, a sinusoidal-shaped step bunch forms for the larger pit structures, which evolve along a qualitatively different path compared to that shown in Figs. 1(a) and 1(d). The insets in Figs. 1(d)–1(h) show high-pass filtered AFM images measured from regions of the surface across pits of the corresponding initial diameters, after the same annealing times. Given the simplicity of the model, the agreement between the length scale dependence of the surface evolution in the simulations and in these experiments is striking.

We extract from the simulated surface morphology both the "in-plane corrugation," which we define as the maximum amplitude of the variation of the steps from straightness within the (111) plane, and the "out-of-plane corrugation," which we define as the amplitude of calculated height profiles across the centers of pits along the staircase direction. These are shown in Figs. 1(g) and 1(j); both nearly exponentially decay with time after the disappearance of the last loop step.

Figure 2 summarizes the relaxation times for both the in-plane and the out-of-plane corrugation as functions of the initial pit diameter, from both the simulations and the experiment.[5] The major features of the size dependence are remarkably well reproduced by this simple model, which neglects the two dimensional nature of the steps. The simulation indicates three regimes of evolution. In the small pattern limit, i.e., for pits of initial diameter smaller than $\sim$2 μm, the in-plane corrugation decays at a rate an order of magnitude faster than that for the out-of-plane corrugation, leading to a rapid relaxation to periodic straight step bunches.[1,5] We note that in this regime the decay times are relatively short, making it difficult to directly experimentally probe. At the

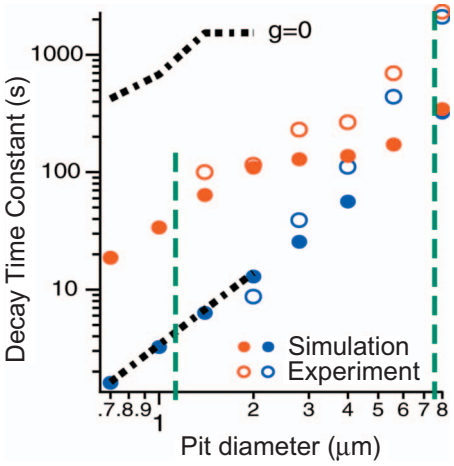

FIG. 2. (Color) Relaxation time constants determined from simulated step structures for in-plane corrugation (filled circles in blue) and out-of-plane corrugation (filled circles in red). For comparison, the open circles show the corresponding experimental measurements (Ref. 5). The dashed curve in black shows the out-of-plane corrugation relaxation time constant for the case of no step-step interaction in the simulation. The two vertical dashed lines show predicted transition points in the size dependence of the pattern, see text for details.

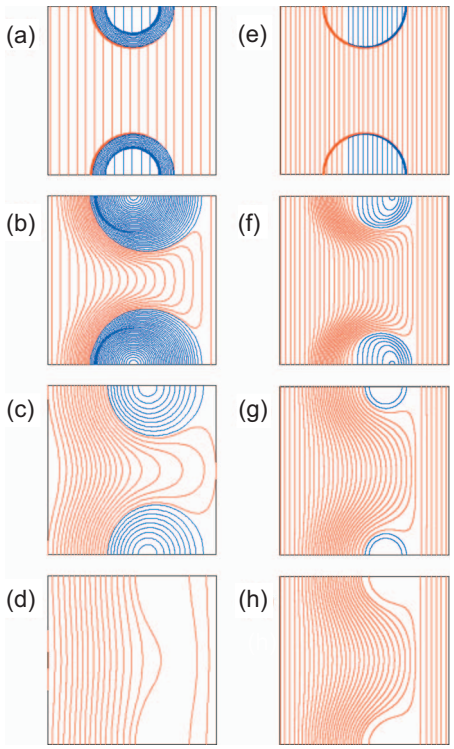

FIG. 3. (Color) Simulated step evolution between pits. The initial pit diameters are 0.7 μm for panels (a)–(d), and 5.6 μm for panels (e)–(h). The field of view panel for (a)–(d) is 1.4 μm, and 11.2 μm for panels (e)–(h). The annealing times for (a)–(d) are 0, 0.5, 2, and 6 s, respectively. For (e)–(h), it is 0, 10, 40, and 60 s, respectively. The step-up direction horizontally points to the left. Again, only a fraction of steps are shown here.

other extreme, for patterns with initial pit diameters larger than ~5.6 μm, the relaxation time for the out-of-plane corrugation converges to that for the in-plane-corrugation. A transition regime occurs for patterns with initial pit diameter between ~2.0 and ~5.6 μm. Here, the out-of-plane corrugation relaxation time does not significantly change, while the in-plane-corrugation relaxation time continues to increase with pit diameter. It is clear from this comparison that the simple step continuum model represented by Eq. (4) successfully captures most of the basic physics governing the self-organized evolution of step bunches on our patterned surfaces.

The evolving step configurations predicted by these simulations provide insights into the origin of the variation in step-bunch self-assembly with pattern size; in particular, an important clue comes from examining the details of the evolving step morphology in the region between pits. Figure 3 shows two cases, corresponding to the two extreme types of behavior seen in Fig. 2. Initially, steps are densely packed in the pit sidewall region. This results in a large frozen-in step-step repulsion energy prior to annealing. After the annealing begins, the strong step-step repulsion drives an expansion of the pit walls, with steps rapidly moving apart in a sort of shock wave. For the small period patterns, the overlap of the individual shock waves from adjacent pits results in significant bending of the vicinal steps. The step stiffness effect associated with the step-bending kicks in to reduce the step length, pulling them straight one by one in the step-up direction and forming a step bunch adjacent to the pit at the uphill side. The overlap of disturbances in step spacing for small period patterns allows relaxation to quickly straighten step bunches after the disappearance of the last loop steps. For the larger period structures, the overlap of the shock waves is not significant, and there is little disturbance to the step spacing at midplanes between pits. Regions of high curvature occur, but the step-step repulsion between closely spaced steps prevents rapid straightening. The steps relax into curved step bunches, maintaining nearly uniform spacing in regions between pits. Figure 3(h) shows that the same trend persists through the disappearance of the loop steps, explaining the formation of sinusoidal shape step bunches experimentally seen.

DISCUSSION

Based on these observations, we can formulate hypotheses for the conditions within this model that set the bounding periods between the different regimes of evolution seen in Fig. 2. For simplicity, we model the shape of the steps of interest to be sinusoidal, e.g., $x=A\sin(2\pi y/L)$, with the period L equal to the center-to-center spacing between the pits, and A the amplitude of step bending. For small pit spacing, the step stiffness dominates the evolution of the step shape and Fig. 3(d) suggests that it is able to keep the steps in the bunch nearly straight between the pits in spite of the increased step-step repulsion (with the loop steps pinning the step bunch before their disappearance). We express this condition below based on Eq. (1):

$$\tilde{\beta}/R \geq gh^3/w_{av}^3, \tag{5}$$

where w_{av} is the average step spacing in bunches between pits. Based on the step configurations seen in Fig. 3(d), as a

rough estimate, we have both w_{av} and A approximately equal to the initial step spacing, i.e., $w_{av} \sim A \sim h/\theta$. Evaluating the maximum curvature of the sinusoidal steps, we determine the lower bounding limit as $L_1 = (2\pi/\theta^2)\sqrt{(h \cdot \tilde{\beta})/g} \sim 2.2$ μm for our values of the energetic parameters and vicinal angle. On the other hand, in the large period limit, the inequality sign in Eq. (5) reverses direction, since the step-step repulsion overrides the step stiffness, maintaining nearly uniform step spacing between pits. The maximum curvature in this case is limited by the maximum amplitude of the step bending between the pit, which in turn is limited by the maximum initial bending of the step possible due to the patterning. This is approximately $d/(2 \sin \theta)$, where d is the initial depth of the pit. This leads to an upper bounding limit of $L_2 = (\pi/\theta^2)\sqrt{(2d \cdot \tilde{\beta})/g} \sim 15.6$ μm for our initial pit depth and vicinal angle. As indicated by the dashed lines in Fig. 2, one-half of L_1 and L_2 approximate the initial diameters which bound the different regimes in the simulation reasonably well. Based on these hypotheses, we predict that the transitions between regimes should be tunable, by varying the vicinal angle and initial pit depth.

In our simulations, we optimized the values of the step parameters in Eq. (4), $\Gamma \cdot \tilde{\beta}$ and $\Gamma \cdot g$, for agreement with experiment; we note that these occur as products, rather than separately. For $\Gamma \cdot g$, we first mapped out the simulated out-of-plane corrugation decay time constant as a function of $\Gamma \cdot g$ for the pit array with a 1.4 μm diameter and a 2.8 μm spacing. We then found that $\Gamma \cdot g = 3.2 \times 10^6$ μm meV/s matches the decay times to those observed in our experimental measurements. To determine $\Gamma \cdot \tilde{\beta}$, we matched the simulated and experimentally measured pit disappearance times, i.e., the time that it takes for all loop steps to annihilate. In this case, we compared results for two pit arrays, one with 1.4 μm diameter and 2.8 μm pitch and the other for pit diameter of 2.0 μm and 4.0 μm pitch. We found that a small window in $\Gamma \cdot \tilde{\beta}$ exists within which the simulation reproduces the observed time sequence of the disappearance of loop steps for these two pit arrays. We choose the middle value of this window, with a value of $\Gamma \cdot \tilde{\beta} = 7.5$ μm^2 meV/s for simulation for the rest of the pit array. Both parameter products, i.e., $\Gamma \cdot \tilde{\beta}$ and $\Gamma \cdot g$, as determined, are 2 orders of magnitude smaller than those extrapolated from equilibrium measurements,[11–14,17] which would be $\Gamma \approx 9 \times 10^6$ nm^3/s, $\tilde{\beta} \approx 90$ meV/nm, and $g \approx 1.4 \times 10^4$ meV/nm^2 at 1273 °C. In spite of these very small values, our numerical simulations show that both of the energetic effects in Eq. (4) are important in comparison to experiment: the dashed curve in Fig. 2 shows that setting the step-step interaction to zero results in a relaxation of the out-of-plane corrugation which is slowed down by more than an order of magnitude. Based on the smoothness of the step edges observed in the experiment and indeed an abnormally large step stiffness reported for Si(111) surface at similar conditions,[15] we deduce that the physical origin of the small magnitudes of $\Gamma \cdot \tilde{\beta}$ and $\Gamma \cdot g$ within this model must result from a large reduction in the far from equilibrium step mobility Γ. Under quasiequilibrium conditions, Γ is equivalent to the amplitude of thermal fluctuations that drives the step fluctuations;[12] this is due to the attachment and detachment of single adatoms from a step, leading to a step mobility which is proportional to the density of diffusing adatoms, both in the diffusion limited and attachment limited cases.[12] A plausible explanation for the very low mobility deduced here would be a depletion of adatom density due to sublimation into vacuum.

An important point at which there is a discrepancy between the simulation and experiment is the power law exponent of the in-plane corrugation relaxation times. The simulated in-plane corrugation and the out-of-plane relaxation times converge to an approximate power law dependence on the length scale for large periods with an exponent of ~ 2, approximately a factor of 2 smaller than that in the experiment.[5] A more realistic model than that defined in Eq. (4), including the step orientation dependence of the step stiffness,[18,19] an integration of the step interactions over their lengths, and interactions beyond near-neighbor steps might resolve this difference. However, we find that setting the interaction strength equal to zero does not alter the predicted power law dependence for in-plane corrugation, as seen in Fig. 2; this indicates that instead the form of the height equation suggested by Weeks *et al.*,[8] must be modified to include a term in the chemical potential which is proportional to the curvature.[10]

In summary, we find that the simple quasi-1D model of step motion proposed by Weeks *et al.*,[8] based on near-equilibrium thermodynamics allows a semiquantitative description of how an artificially introduced pattern directs the self-organization of step bunches during annealing of Si(111). Within this model, in the small period limit, the step stiffness dominates the evolution, while in large period limit, the step-step interaction takes over. The transition length scales are seemingly controlled by the vicinal angle and pattern depth. A detailed quantitative comparison between the model and experiments show that the interaction parameters used to describe steps on Si(111) at high temperatures must vary considerably from their equilibrium values. Finally, our comparison indicates that a detailed, quantitative description of the self-organization of step bunches will require a modification in the functional form of the simple model examined.

ACKNOWLEDGMENTS

This work was supported by the Laboratory for Physical Sciences and the NSF-MRSEC at the University of Maryland, DMR 0520471. We thank N. C. Bartelt and A. Pimpinelli for helpful discussions.

*Present address: Department of Physics, National Chung Cheng University, Chia-Yi, Taiwan, Republic of China.

[1] T. Ogino, Y. Homma, Y. Kobayashi, H. Hibino, K. Prabhakaran, K. Sumitomo, H. Omi, S. Suzuki, T. Yamashtia, D. J. Bottomley, F. Ling, and A. Kaneko, Surf. Sci. **514**, 1 (2002).

[2] S. Tanaka, N. C. Bartelt, C. C. Umbach, R. M. Tromp, and J. M. Blakely, Phys. Rev. Lett. **78**, 3342 (1997).

[3] D. Lee, J. M. Blakely, Todd W. Schroeder, and J. R. Engstrom, Appl. Phys. Lett. **78**, 1349 (2001).

[4] A. Dalla Volta, D. D. Vvedensky, N. Gogneau, E. Pelucchi, A. Rudra, B. Dwir, E. Kapon, and C. Ratsch, Appl. Phys. Lett. **88**, 203104 (2006).

[5] T. Kwon, R. J. Phaneuf, and H.-C. Kan, Appl. Phys. Lett. **88**, 071914 (2006).

[6] H.-C. Kan, S. Shah, T. Tadayyon-Eslami, and R. J. Phaneuf, Phys. Rev. Lett. **92**, 146101 (2004).

[7] H.-C. Kan, R. Ankam, S. Shah, K. M. Micholsky, T. Tadayyon-Eslami, L. Calhoun, and R. J. Phaneuf, Phys. Rev. B **73**, 195410 (2006).

[8] J. D. Weeks, D.-J. Liu, and H.-C. Jeong, in *Dynamics of Crystal Surfaces and Interfaces*, edited by P. Duxbury and T. Spence (Plenum, New York, 1997), pp. 199–216.

[9] E. E. Gruber and W. W. Mullins, J. Phys. Chem. Solids **28**, 875 (1967).

[10] W. W. Mullins, J. Appl. Phys. **30**, 77 (1959).

[11] J. J. Metois, J. C. Heyraud, and S. Stoyanov, Surf. Sci. **486**, 95 (2001).

[12] N. C. Bartelt, J. L. Goldberg, T. L. Einstein, E. D. Williams, J. C. Heyraud, and J. J. Metois, Phys. Rev. B **48**, 15453 (1993).

[13] S. D. Cohen, R. D. Schroll, T. L. Einstein, J.-J. Metois, H. Gebremariam, H. L. Richards, and E. D. Williams, Phys. Rev. B **66**, 115310 (2002).

[14] E. S. Fu, M. D. Johnson, D.-J. Liu, J. D. Weeks, and E. D. Williams, Phys. Rev. Lett. **77**, 1091 (1996).

[15] A. V. Latyshev, H. Minoda, Y. Tanishiro, and K. Yagi, Phys. Rev. Lett. **76**, 94 (1996).

[16] G. Ehrlich and F. G. Hudda, J. Chem. Phys. **44**, 1039 (1966); R. L. Schwoebel and E. J. Shipsey, J. Appl. Phys. **37**, 3682 (1966).

[17] W. K. Burton, N. Cabrera, and F. C. Frank, Philos. Trans. R. Soc. London, Ser. A **243**, 299 (1951).

[18] S. Dieluweit, H. Ibach, M. Giesen, and T. L. Einstein, Phys. Rev. B **67**, 121410(R) (2003).

[19] T. J. Stasevich and T. L. Einstein, Multiscale Model. Simul. **6**, 90 (2007).